Glycoconj J (2010) 27:445–459
DOI 10.1007/s10719-010-9292-3

Development of delivery methods for carbohydrate-based drugs: controlled release of biologically-active short chain fatty acid-hexosamine analogs

Udayanath Aich · M. Adam Meledeo · Srinivasa-Gopalan Sampathkumar · Jie Fu · Mark B. Jones · Christopher A. Weier · Sung Yun Chung · Benjamin C. Tang · Ming Yang · Justin Hanes · Kevin J. Yarema

Received: 19 January 2010 / Revised: 10 April 2010 / Accepted: 14 April 2010 / Published online: 11 May 2010

Abstract Carbohydrates are attractive candidates for drug development because sugars are involved in many, if not most, complex human diseases including cancer, immune dysfunction, congenital disorders, and infectious diseases. Unfortunately, potential therapeutic benefits of sugar-based drugs are offset by poor pharmacologic properties that include rapid serum clearance, poor cellular uptake, and relatively high concentrations required for efficacy. To address these issues, pilot studies are reported here where 'Bu_4ManNAc', a short chain fatty acid-monosaccharide hybrid molecule with anti-cancer activities, was encapsulated in polyethylene glycol-sebacic acid (PEG-SA) polymers. Sustained release of biologically active compound was achieved for over a week from drug-laden polymer formulated into microparticles thus offering a dramatic improvement over the twice daily administration currently used for *in vivo* studies. In a second strategy, a tributanoylated ManNAc analog (3,4,6-*O*-Bu_3ManNAc) with anti-cancer activities was covalently linked to PEG-SA and formulated into nanoparticles suitable for drug delivery; once again release of biologically active compound was demonstrated.

Keywords Carbohydrate drug delivery · SCFA-hexosamine analogs · PEG-SA polymer · Microparticles · Nanoparticles

Udayanath Aich, M. Adam Meledeo, Srinivasa-Gopalan Sampathkumar and Jie Fu contributed equally.

Electronic supplementary material The online version of this article (doi:10.1007/s10719-010-9292-3) contains supplementary material, which is available to authorized users.

M. A. Meledeo · M. B. Jones · C. A. Weier · S. Y. Chung · M. Yang · K. J. Yarema (✉)
Department of Biomedical Engineering,
The Johns Hopkins University,
Clark Hall 106A, 3400 North Charles Street,
Baltimore, MD 21218, USA
e-mail: kyarema1@jhu.edu

J. Fu · B. C. Tang · J. Hanes
Department of Chemical and Biomolecular Engineering,
The Johns Hopkins University,
Baltimore, MD, USA

Present Address:
U. Aich
Department of Biological Engineering,
Massachusetts Institute of Technology,
Cambridge, MA 02139, USA

Present Address:
S.-G. Sampathkumar
Laboratory of Chemical Glycobiology,
National Institute of Immunology Aruna Asaf Ali Marg,
New Delhi 110067, India

Abbreviations

PEG	poly(ethylene glycol)
poly(PEG-SA)	poly(polyethylene glycol-co-sebacic anhydride)
poly(PEG-SA):**1**	Compound **1** (Bu_4ManNAc) non-covalently encapsulated in poly(PEG-SA)
polySA-**2**	Compound **2** (3,4,6-*O*-Bu_3 ManNAc) covalently linked to polySA-**2**
polySA-**2**-NP	nanoparticles formulated from polySA-**2**
PVA	poly(vinyl alcohol).
AUC	area under the curve

Introduction

Therapeutic applications for carbohydrates have attracted increased attention in recent years. A high profile example is heparin, a well established anticoagulant that has been beset with quality control issues, in part because it is a complex mixture of high molecular weight molecules, isolated from natural sources, that can obscure contaminants such as over-sulfated chondroitin sulfate [1]. At the opposite end of the spectrum from polysaccharides isolated from natural sources are small molecule carbohydrate-based drug candidates (often chemically-modified monosaccharides) that can be synthesized and fully characterized. Unfortunately, these molecules have long been plagued with a reputation for being "undruggable" due to inferior pharmacokinetic properties, poor bioavailability, fast serum clearance, and rapid degradation. Counter to conventional wisdom, however, compelling evidence has now accumulated that this class of molecules is a surprisingly versatile platform for drug discovery (as discussed in detail in a recent review [2]).

Recent work from our laboratory, exemplified by butanoylated *N*-acetylmannosamine (ManNAc) analogs (*e.g.*, compounds **1**, **2**, and **3**, Fig. 1a), supports the premise that a simple sugar can modulate biological activity when properly functionalized [3]. These efforts arose from experiments that found that analogs used in metabolic glycoengineering [4, 5] had unique biological activities depending on the type and regioisomeric positioning of ester-linked short chain fatty acid (SCFA) originally installed to increase the cellular uptake of the sugar [6, 7]. In particular, the tributanoylated ManNAc isomers **2** and **3** have dramatically different activities [8] wherein **2** mimics the parent perbutanoylated analog **1** by exhibiting a suite of anti-cancer effects that include induction of apoptosis, inhibition of NF-κB, and suppression of pro-invasive oncogenes [9–11]. By contrast, **3** has none of these properties but instead supports a high rate of flux through the sialic acid biosynthetic pathway [8]; this attribute is favorable for metabolic glycoengineering experiments where the goal is to supplement a targeted glycosylation pathway with exogenously-supplied metabolites to enhance the expression of natural glycans [12] or to install non-natural glycans on the cell surface [4, 13, 14].

Based on their favorable *in vitro* properties, **1** and **2** are attractive cancer drug candidates provided that potential obstacles to *in vivo* testing and ultimately, to clinical translation, can be overcome. At the outset, the ester-linked *n*-butyrate groups of these compounds had already solved a significant challenge of therapeutic carbohydrates; namely, slow cellular uptake due to membrane impermeability of these highly hydrophilic compounds. Instead, **1** and **2** [8]—following the trend set by other short chain fatty acid (SCFA)—modified sugars [14, 15]—are efficiently taken up

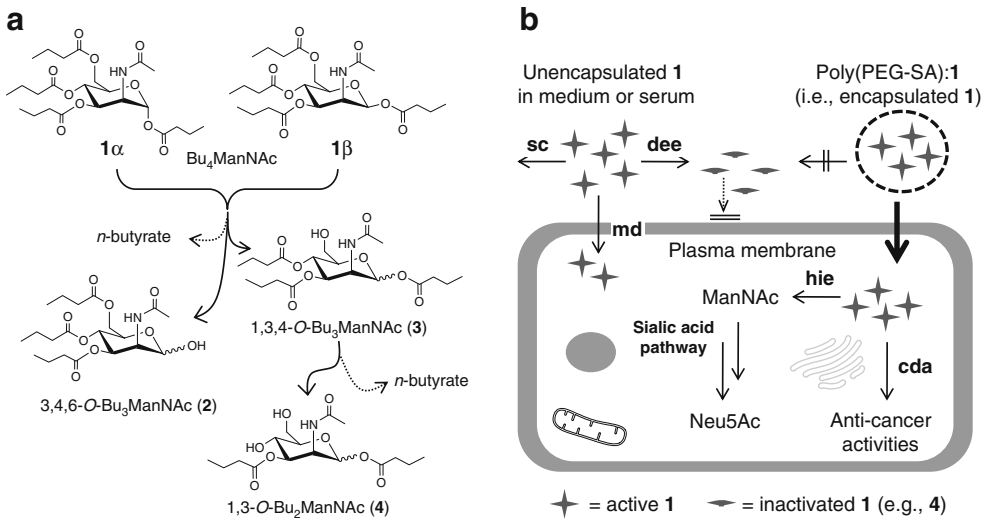

Fig. 1 Strategies for the encapsulation of butanoylated ManNAc species in poly(PEG-SA). **a** The alpha (α) and beta (β) configurations of Bu_4ManNAc (1) are shown; throughout this study an ~1:10 α:β anomeric mixture was used. Extra- or intra-cellular esterases hydrolyze *n*-butyrate from **1** producing 3,4,6-*O*-Bu_3ManNAc (**2**), a compound with anticancer activities that includes induction of apoptosis [6] and suppression of pro-invasive oncogenes [5], or 1,3,4-*O*-Bu_3ManNAc (**3**), a compound that supports high level of metabolic flux through the sialic acid pathway with negligible toxicity [4]. Further hydrolysis of **3** into **4** (or other diacylated species) functionally inactivates the compound by dramatically reducing flux into the sialic acid pathway by reducing membrane diffusion (*i.e.*, "md" in panel b). **b** Bu_4ManNAc (**1**, panel a) is subject to serum clearance ("sc") or degradation by extracellular esterases ("dee"); these competing reactions hinder membrane transport ("md") and internalization of **1** by the target cell. Encapsulation of **1** in poly(PEG-SA) (as poly(PEG-SA):**1**) reduces "sc" and "dee" thereby facilitating membrane transport. Once inside a cell, **1** can support cancer drug activity ("cda") or be hydrolyzed by intracellular esterases ("hie") producing ManNAc that is converted into sialic acid (*e.g.*, *N*-acetylneuraminic acid, Neu5Ac)

by cells *in vitro* as shown by "md"—representing "membrane diffusion"—in Fig. 1, panel b due to the increased lipophilicity of these hybrid molecules [7]. Cellular uptake could be compromised *in vivo*, however, if **1** was partitioned to competing targets through serum clearance ("sc") or degraded by extracellular esterases ("dee") creating membrane impermeable compounds such as **4** (Fig. 1, panel b). Experimental evidence that factors such as these that limit the serum longevity of active compound was provided by *in vivo* testing of peracetylated *N*-propanoylmannosamine (Ac_4ManNPr, which like **1** and **2** is a SCFA-hexosomine hybrid molecule) by Gagiannis and coworkers in studies that required cumbersome twice a day dosing regimens over a 6 week period [16].

In the current study, we reasoned that factors that limit the bioavailability or reduce the serum longevity of monosaccharide-based drug candidates could be ameliorated by encapsulating these compounds in a biodegradable polymer for controlled release. This strategy would concurrently provide protection from degradative enzymes and ultimately could be exploited to target the drug to a diseased cell or tissue upon proper formulation into nano- or microparticles. Accordingly, the first goal of this study was to create biomaterials capable of stable encapsulation and sustained release of biologically-active *n*-butanoylated hexosamines such as **1** or **2** over multiple days. To accomplish this objective, we used polyethylene glycol (PEG) sebacic anhydride (SA) copolymers (poly(PEG-SA), see Fig. 6 below) [17] to encapsulate **1** into microspheres and developed HPLC-based methods to monitor its release. To ensure maximum versatility for this emerging technology, and take advantage of growing interest in therapeutic nanoparticles [18], we covalently-linked **2** to poly(PEG-SA) to create a material suitable for formulation into nanoparticles. Finally, by testing endpoints that included the activation of sialic acid production and the suppression of pro-invasive oncogenes, we verified the biological activity of both polymer-encapsulated **1** and nanoparticle-formulated **2**.

Results and discussion

HPLC quantification of Bu_4ManNAc release from polymer

At the outset of this study, HPLC conditions were optimized for anomer peak separation allowing two peaks to be identified, at R_t of 4.427 min and 5.221 min, corresponding to **1β** and **1α**, respectively (Fig. 2, panel a). The ratio of the relative *area under the curve* (AUC) for **1β** and **1α** was 90/10, which was identical to the ratio obtained by ^{1}H-NMR [7]. The total AUC of both anomers **1β** and **1α** were combined and the calibration curve based on a series of dilutions in acetonitrile was linear with excellent correlation for the AUC up to 10 mg/mL of **1** (Fig. 2, panel b) indicating that this concentration range was appropriate for characterization of the **1** in the controlled released experiments described below.

Bu_4ManNAc release from polymer (*i.e.*, poly(PEG-SA):**1**) was not limited by solubility

In order to estimate the solubility of **1** under aqueous (*i.e.*, physiologically-relevant) conditions to ensure that the release studies would not be confounded by the solubility limit, a suspension of **1** (10 mg) in PBS (1.0 mL) was incubated at 37°C for 16 h with mixing, in order to achieve (and then measure) saturating solubility. At the end of this time period, excess (*i.e.*, undissolved) **1** was observed as immiscible liquid droplets in the PBS that did not diminish further in size with time; aliquots of the soluble portions were carefully removed by syringe needle and analyzed by HPLC. The resulting unknown concentration was estimated by using the calibration curve developed above (shown superimposed on a portion of the curve from Fig. 2, panel b in panel c). By using this method, the saturating solubility of **1** in PBS under conditions similar to those subsequently used to quantify controlled release of analog from poly(PEG-SA):**1** was found to be ~0.40 mg/mL at 37°C (panel d), corresponding to a concentration of ~800 μM. Because this analog concentration was not achieved during release studies despite a longer incubation period (*e.g.*, ~24 h compared to 16 h), it was deduced that particle degradation and not solubility primarily controlled release kinetics. Furthermore, the relative ratio of anomers (**1β** / **1α**) was conserved in PBS indicating that there was no stereochemical preference for the encapsulation or release of either anomer into an aqueous medium.

Encapsulation of Bu_4ManNAc (**1**) in poly(PEG-SA) and formulation into microspheres

In the next part of this study, drug-laden microparticles were prepared using poly(PEG-SA):**1** at theoretical loading ratios of 70:30 and 80:20 of PEG-SA polymer:**1** by weight. The size of the particles was determined to be ~8 μm in diameter by using a Coulter Multisizer IIe [17] and the actual loading ratios were determined by HPLC quantification to be 22% and 12% of **1** for the 70:30 and 80:20 formulations, respectively, (as described in the next section, below). After the total amount of **1** that was released was determined, these values correspond to encapsulation efficiencies of 73% and 60% respectively. It should be noted that only perbutanoylated compound was quantified; therefore if tributanoylated or dibutanoylated (or further hydrolyzed derivatives of **1** such as **2**, **3**, or **4**, see Fig. 1, panel a) had been formed during the process, the actual

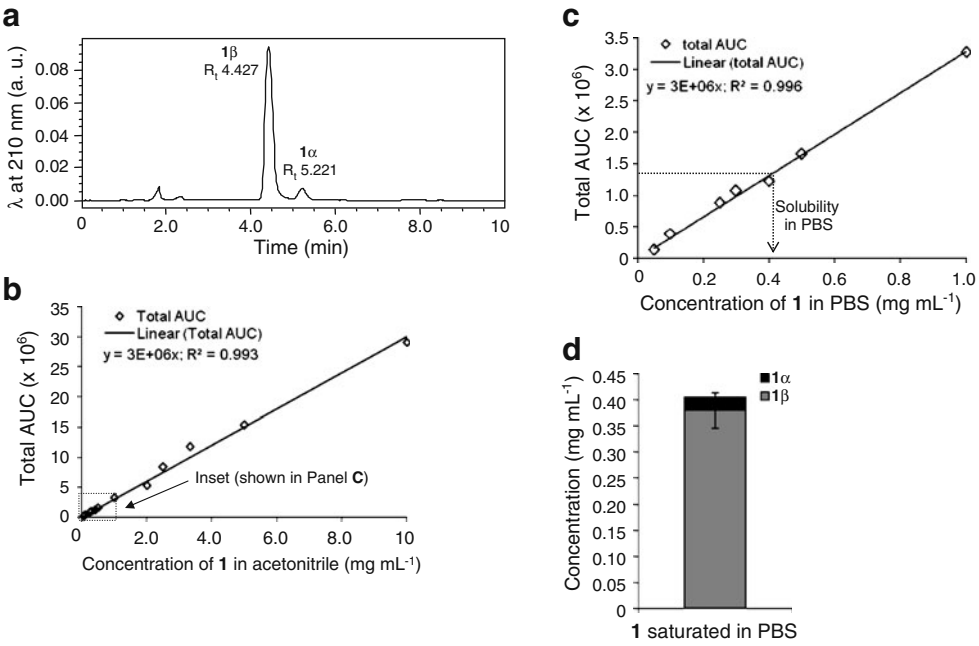

Fig. 2 Methodology for quantifying Bu_4ManNAc (1). **a** HPLC elution profiles show the separation of α and β anomers of **1**. **b** A standard curve for the quantification of **1** was determined from HPLC traces as shown in Panel **a** (AUC = area under curve). **c** The method used to quantify **1** recovered from the daily release of encapsulated analog by HPLC is shown. The AUC from an aliquot of released material is superimposed on the lower portion of the curve from Panel **b**. **d** The solubility limit of **1** (showing the proportions of recovered α and β anomers) was determined after equilibrium was achieved upon adding 10 mg of **1** to 10 mL of PBS at 37°C

encapsulation efficiency of analog would be higher. However, we established that **1** was stable under assay conditions (*e.g.*, in PBS at R.T. or 37°C) indicating that the lower than theoretical encapsulation efficiencies of 73% and 60% are most likely due to the loss of soluble **1** in the mother liquor during encapsulation and microparticle formation.

Characterization of Bu_4ManNAc (**1**) release from poly (PEG-SA):**1** microparticles

To study the controlled release of encapsulated **1** from poly (PEG-SA):**1** under aqueous conditions, 10 mg of microparticles were suspended in 1.0 mL of PBS at 37°C in three replicate samples. At regular intervals (once every 24 h for 14 days) the supernatant containing released **1** (along with soluble polymer degradation products) were collected after centrifugation. The pellet containing the non-degraded microparticles was then re-suspended in fresh PBS for sample collection on subsequent days and aliquots of the supernatants collected each day were analyzed by HPLC. For microparticles with 30% theoretical (~22% actual) loading (Fig. 3, panel a), the supernatants from day 1 to day 5 contained **1** at concentrations ranging from 0.30 mg/mL to 0.34 mg/mL, followed by a gradual decrease in release form day 6 to day 10. The concentration of **1** in the PBS supernatants was lower than previously-determined saturation limit of 0.4 mg/mL (which had been determined at a shorter time point) ensuring that the equilibrium kinetics of solubility were not limiting the release of analog from the polymer.

The microparticles prepared with 30% theoretical loading exhibited well-behaved linear controlled release kinetics that avoided an initial burst but instead maintained nearly constant release of **1** over each 24 h interval during the first 6 days followed by diminishing release up to day 12. This release profile was consistent with a surface eroding mechanism for poly(PEG-SA):**1** microparticle degradation, as expected for polyanhydride polymers [19]. By comparison, the 20% theoretically-loaded particles released a peak amount of **1** on day 2 followed by decreasing amounts until day 7 (Fig. 3, panel b); the difference in release is likely simply the lower amount of actual incorporation (12% v. 22%) of **1** in the 20:80-loaded polymer. As mentioned, an important feature of the HPLC analysis utilized for quantification of released **1** was the ability of this method to resolve the ratio of the two anomers (**1β** and **1α**). The ratio of 90/10 for β/**α** was conserved in the released supernatants for all time points (Fig. 3, panel c) indicating that both the anomers were encapsulated and released at similar rates. Although not pursued further in this work, if future studies show that the β and **α** isomers of SCFA-ManNAc analogs have distinct biological activities, these findings ensure that the delivery systems developed here will be applicable for both anomers.

Biological activity was retained for Bu_4ManNAc (**1**) released from poly(PEG-SA):**1**

Drugs undergoing controlled release are customarily evaluated to ensure that they retain the biological activity of the unconjugated drug and lack undesired side effects from degradation products. Accordingly, having confirmed the controlled release of **1** encapsulated in poly(PEG-SA) microparticles (as shown in Fig. 3) over a period of greater

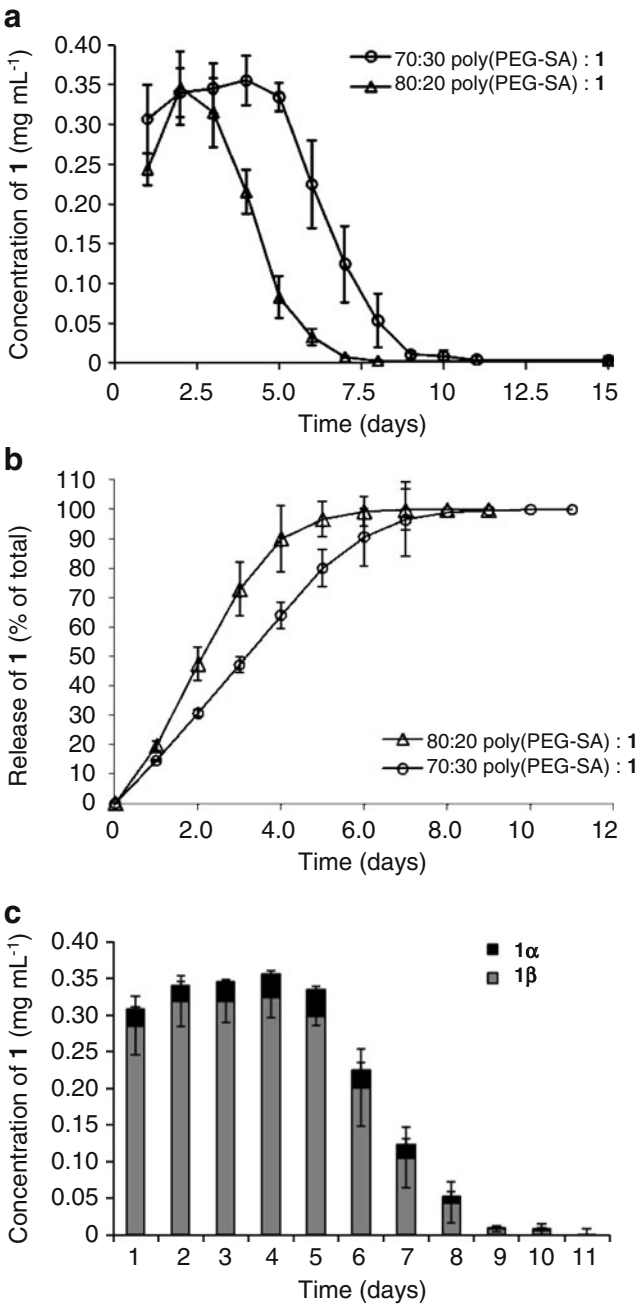

Fig. 3 Controlled release of Bu_4ManNAc from poly(PEG-SA):1. **a** Supernatants from microparticles formulated from poly(PEG-SA):**1** and incubated in PBS were collected each day and quantified by the HPLC method described in Fig. 2; the amount of **1** released each day is shown. **b** A plot of cumulative amounts of **1** recovered from poly (PEG-SA):**1** supernatants each day shows that release is essentially complete after ~5 days for the 80:20 formulation and ~8 days for the 70:30 formulation. **c** The relative amounts of α and β anomers of **1** released each day remains constant. In each case, error bars represent SEM with $n \geq 3$

than 1 week, we next tested the biological activity of released **1** to verify that the structural integrity of this compound was preserved during the microparticle preparation and subsequent release. The endpoint evaluated in the first of these experiments was sialic acid production employing a functional assay described previously [20]. Sialic acid production in "indicator cells", in this case Jurkat cells, provides a sensitive and linear readout of exogenous ManNAc concentrations, provides a measure of the complete metabolic processing of **1** to ManNAc, because all four ester groups must be hydrolyzed to produce the free hydroxyl form of this sugar that serves as a metabolic precursor for sialic acid biosynthesis. Moreover, ManNAc is a committed intermediary for sialic acid biosynthesis with no other known metabolic fates [21, 22]; therefore an increase in cellular levels of this sugar provides both unambiguous and quantitative evidence for the release of biologically active **1** from poly (PEG-SA):**1** microspheres.

As a positive control for sialic acid production, the indicator cells were treated with unconjugated **1** at concentrations that matched the amount of **1** in the supernatants obtained from PBS-incubated poly(PEG-SA):**1** as determined by the HPLC quantification method described above. To explain this process using Day 5 data (see Fig. 4, panel a) as an example, the supernatant obtained from particles on this day was found to contain 670 μM of **1** by HPLC. A 1:10 dilution of this supernatant was added to the culture medium of the indicator cells giving a theoretical final concentration of 67 μM of **1**. Therefore, in a parallel experiment, cells were incubated in media containing 67 μM of a stock solution of unencapsulated **1** as a positive control to determine the expected amount of sialic acid production. Finally, in a control experiment (data not shown), the addition of 10% volume of PBS to the culture medium did not alter the growth rates or endogenous sialic acid production by the cells, consistent with previous findings [20].

By following this procedure, cells were incubated either with a series of PBS supernatants containing **1** from the controlled release experiments that were diluted 1:10 in cell culture medium or with stock **1** at concentrations corresponding to 10% of that expected to be found in the supernatants. After 48 h, the cells were harvested and analyzed for total sialic acid content using the periodate-resorcinol assay (Fig. 4, panel a). The supernatants from days 1, 3, 5 and 7 all exhibited ~70–90% of activity in terms of sialic acid production compared to stock **1**, indicating that the biological activity of **1** largely was preserved during microparticle encapsulation and subsequent controlled release over extended periods of time. Furthermore, the slight decrease in activity that was observed was constant over time suggesting that the loss in activity occurred during the encapsulation process rather than during the extended release period, in which case progressively decreasing levels of activity would have been expected from batches isolated on subsequent days.

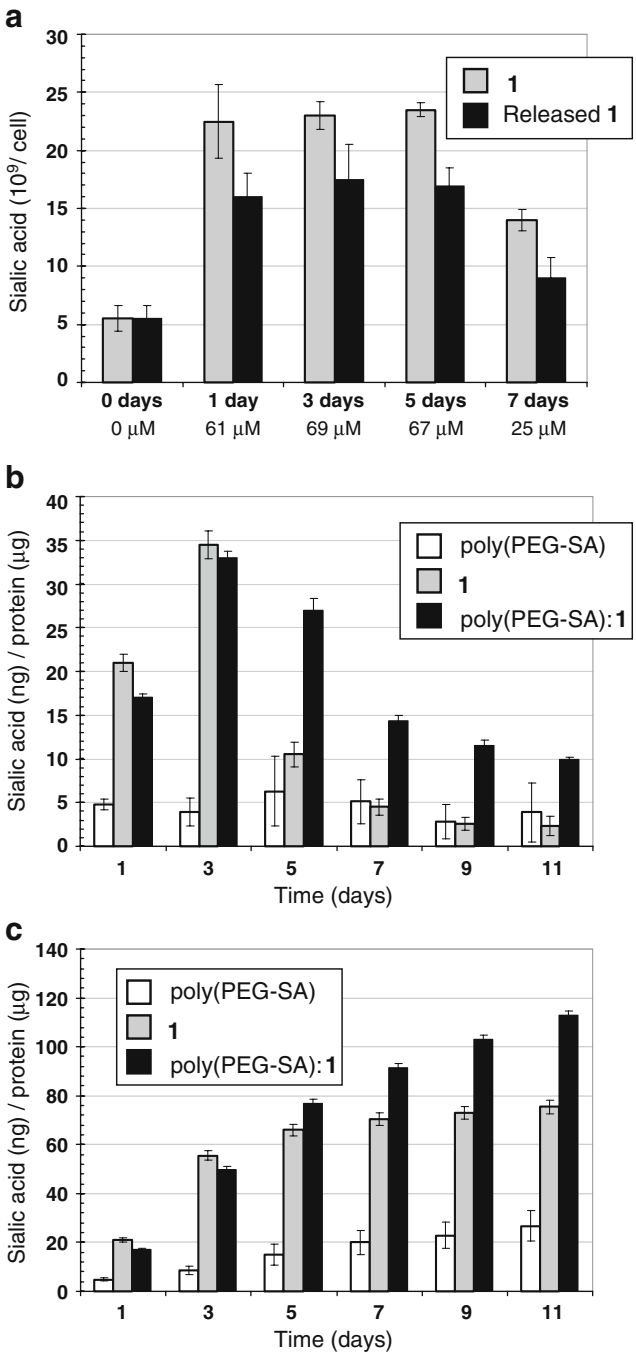

Fig. 4 Sialic acid production from poly(PEG-SA):1. **a** Sialic acid production was monitored in Jurkat cells incubated with **1** recovered from supernatants of poly(PEG-SA):**1** that had been incubated with PBS over the indicated number of days (as shown in Fig. 3). In addition, a stock solution of unencapsulated **1** was tested (as the positive control) at concentrations that matched the amount of **1** recovered from the supernatants. **b** Sialic acid production in Jurkat cells co-incubated with microparticles of poly(PEG-SA):**1**, unladen poly(PEG-SA) (the negative control), or unencapsulated **1** (the positive control). In this experiment, the test compounds were added once (on day 0) and measurements of sialic acid were made at the indicated time points. **c** Cumulative levels of sialic acid produced by a normalized number of cells (as determined by protein content) from Panel **b** are shown. Error bars represent SEM with $n \geq 3$

The biological activity of poly(PEG-SA):**1**—measured by sialic acid production—was retained in tissue culture conditions

Ultimately, for controlled release to be useful *in vivo*, the delivery method must be compatible with (and able to withstand) physiological conditions; the first step towards demonstrating this compatibility occurred by showing the controlled release of active **1** into aqueous solution (*i.e.*, PBS) as described above. This experiment, however, did not include the complicating effects of esterases or lipases that are present in serum that are capable of degrading and inactivating **1** before uptake by cells (as indicated by "dee" in Fig. 1, panel b). Accordingly, we next demonstrated that extended release of biologically active **1** was compatible with the presence of serum by incubating the microparticles directly with Jurkat cells in serum-containing medium. The sialic acid levels determined from cells incubated with poly (PEG-SA) microparticles remained unchanged over the 11 day assay period indicating that the polymer and its degradation products did not compromise the endogenous sialic acid biosynthetic pathway (Fig. 4, panel b, white bars). By comparison, treatment of cells with unencapsulated **1** increased sialic acid production dramatically (up to 7 to 9-fold over endogenous levels) during the initial 3 days of treatment followed by a rapid decline to background levels by day 5 and day 7 (gray bars). The transient increase in sialic acid expression indicated that **1** was efficiently internalized by cells, hydrolyzed to free ManNAc by intracellular esterases and processed by the sialic acid pathway (as outlined in Fig. 1, panel a). Unlike unencapsulated **1**, sialic acid production from an equivalent mass of **1** supplied as poly (PEG-SA):**1** was maintained at a high level on day 5 and was then sustained at levels significantly above background until day 11 (Fig. 4, panel b, solid bars). The cumulative benefit of poly(PEG-SA):**1** compared to unencapsulated **1** was not only manifest in a *longer* period of elevated sialic acid production, but also in an increased *total amount* of sialic acid produced for a given number of cells (Fig. 4, panel c).

Several factors likely contributed to the rapid decrease in sialic acid levels in cells exposed to unencapsulated **1** after 3 days. First, a proportion of the analog was converted into sialic acid resulting in substrate depletion; this factor did not fully explain the diminished sialic acid production, however, as an accounting of analog added to the cells compared with the amount of sialic acid actually produced (by methods described in detail elsewhere [20]) revealed that even under optimal conditions less than 50% of the analog was converted into sialic acid. Instead, under routine conditions large amounts (80% or more) of analog was simply "missing" having been removed from the medium

but not appearing as pathway metabolites. The ability of poly(PEG-SA)-**1** to support higher levels of sialic acid production compared to unencapsulated **1** could arise from two benefits of controlled release. One explanation is that controlled release diminishes the portion of compound that becomes non-productively sequestered in intracellular reservoirs—for example it could partition into lipid bilayers due to its lipophilicity, thereby rendering the compound inaccessible to pathway enzymes [20]. A second possibility was that **1** was inactivated by extracellular serum esterases ("dee" in Fig. 1, panel b; the removal of two *n*-butyrate groups of **1** (*e.g.*, exemplified by **4**, Fig. 1, panel a) severely limits the biological activity of **1** due to restricted membrane permeability) and encapsulation provides protection from this mode of analog inactivation.

Growth inhibition was enhanced by sustained release of **1** from poly(PEG-SA):**1**

As described above, sialic acid production verified that **1** released from poly(PEG-SA):**1** retained biological activity. A second and complementary endpoint was provided by the other functional group of **1** (*i.e.*, *n*-butyrate), which has anti-cancer potential as a histone deactylase inhibitor (HDACi) [10]. HDACi up-regulate the cell cycle check-point protein p21 (as well as other genes [23]) and subsequently inhibit the growth of cancer cells and in some cases induce apoptosis. Previous efforts to kill or inhibit the growth of cancer cells with sugar-delivered SCFA have proven challenging, however, the cells recover from a single application of drug and resume rapid growth after several days [10]. Therefore, it was intriguing that poly (PEG-SA):**1** had enhanced cytotoxicity (compared to **1** or unladen poly(PEG-SA), Fig. 5, panel a), suggesting that sustained application of a given amount of **1** was more toxic to cancer cells than an equivalent amount given as a single bolus.

To verify the premise that sustained release of otherwise sub-cytotoxic amounts of **1** from poly(PEG-SA):**1** could potently inhibit cancer cell growth, Jurkat cells were incubated with unencapsulated **1** corresponding to the release profile shown in Fig. 4, panel a (specifically, 61 μM on day 1, 69 μM on day 3, 67 μM on day 5, 25 μM on day 7, and 0 μM on day 9). In this experiment, repeated doses of **1** that simulated the sustained release of **1** from poly(PEG-SA):**1** gave a toxicity profile similar to that obtained from a single exposure of cells to poly(PEG-SA):**1** (Fig. 5, panel b). These results, together with the enhanced sialic acid production reported above, establish polymer-based delivery as a superior method (compared to unencapsulated analog) for both high flux, non-toxic compounds such as **3** [8, 24] and for apoptosis-inducing, anti-invasive cancer drug candidates such as **2** [8, 9], depending on the intended application.

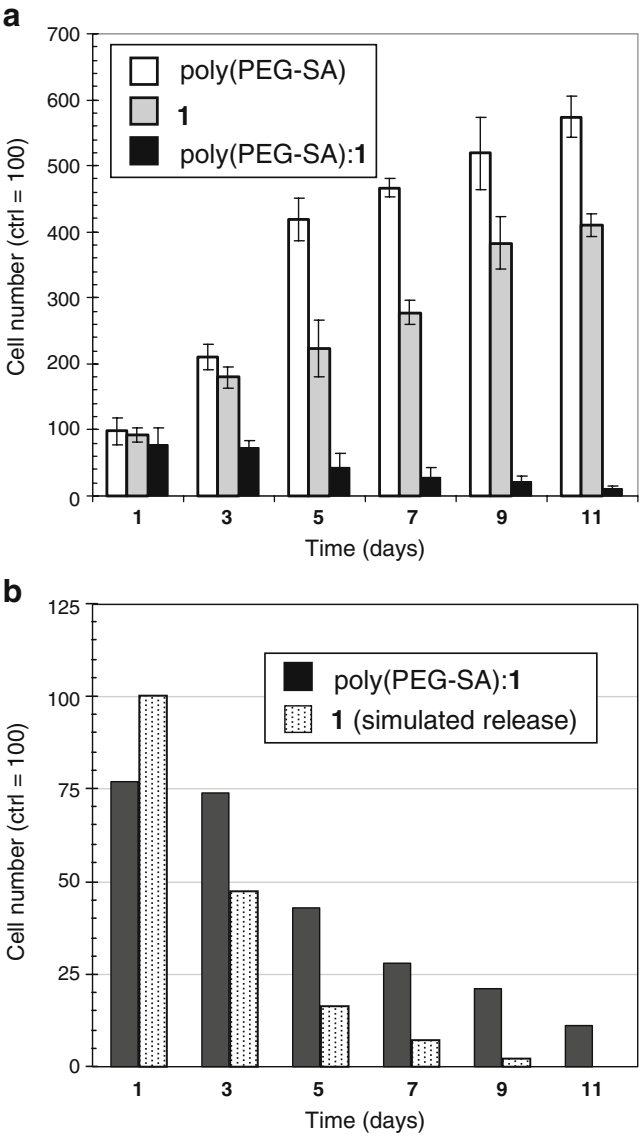

Fig. 5 Growth inhibitory effects of poly(PEG-SA):1 in cancer cells. **a** PEG-SA:**1** suppressed the growth of Jurkat cells whereas equivalent concentrations of **1** slowed growth only slightly; as a control, unladen poly(PEG-SA) (shown) did not alter growth rates compared to grown cells with no test agent added to the culture medium (not shown). In this experiment, the test compounds were added once (on day 0) and cell number was monitored at the indicated time points. **b** Controlled release of **1** from poly(PEG-SA):**1** was mimicked by day-to-day addition of matched concentrations of unencapsulated **1**, showing that prolonged exposure to otherwise sub-cytotoxic levels of unencapsulated analog resulted in long-term growth suppression. This data (*gray bars*) is shown along with the poly(PEG):**1** data from Panel a (*black bars*) for comparison purposes. Error bars represent SEM, $n \geq 3$

Synthesis of polySA-**2**

To further increase the versatility of biopolymer-delivered sugar analogs, we next sought to extend delivery technologies to nanoparticles, which are attracting increased scrutiny for therapeutic applications [18]. At the outset, we were

concerned that diffusion of **1** from a nanoparticle (which would be much more rapid on a per molecule basis compared to microparticles because of the larger surface to volume ratio of the smaller particles) would thwart the delivery of a sufficiently drug-laden entity to a specific target in the body. To ensure sufficient stability to allow a particle to remain intact for several hours, we took advantage of the structure activity relationships (SAR) alluded to above where the SCFA attached to the C1-OH group of **1** was not required for the anti-cancer activities of this molecule [8] (in fact, the tributanoylated analog **2**, (Fig. 1, panel a) had improved anticancer activities compared to **1**, which included enhanced induction of apoptosis and suppression of pro-invasive oncogenes [9, 10, 23]) to covalently link the **2** to poly(PEG-SA) by using the strategy depicted in Fig. 6.

Characterization of polymer conjugates

Structural characterization of **2** by NMR spectroscopy before and after (as polySA-**2**) conjugation to polymer are shown in Fig. 7 and representative NMR and IR spectra are also shown in the Supplementary Material (Figs. S4–S8). The presence of conjugated analog was verified by the chemical shift of the anomeric proton in the ^{1}H-NMR spectrum of polySA-**2** from 6.03 ppm and 5.86 ppm, respectively, for the anomers of unconjugated **2** compared to the value of 5.25–5.00 ppm after esterification and conjugation to polymer. The peaks at 2.55–2.10, 1.78–1.50, 1.45–1.20 in the 1H-NMR spectrum are due to the CH_2 hydrogen of polymer and ester alkyl group of SCFA-ManNAc (Fig. 7, panel b) as expected. Similarly, a differential chemical shift was observed in ^{13}C-NMR spectra, where polymer conjugates showed C-1 chemical shift at 91.6 ppm and 90.7 ppm instead of 94.0 and 93.7 for **2**, due to esterification of C1 hydroxyl group. From the NMR chemical shift integration values it was calculated that polySA-**2** was 16% sugar analog by weight. After polySA-**2** was shown to have growth inhibitory and cytotoxic properties characteristic of **2** (as described below), nanoparticles were prepared from polySA-**2** (as well as unconjugated polymer) by using the single emulsion solvent method. The sizes of the resulting nanoparticles were 162.4±14.3 and 185.5±34.1 nm for polySA-**2**-NP and polySA-NP, respectively.

3.10. Cytotoxicity of polySA-2 in Jurkat cells and formulation into nanoparticles

To verify that polySA-**2** retained the biological activities of **2**, two concerns had to be addressed. First, the temperatures required during synthesis had the potential to inactivate the analog; this concern was largely allayed through the structural characterization that revealed no

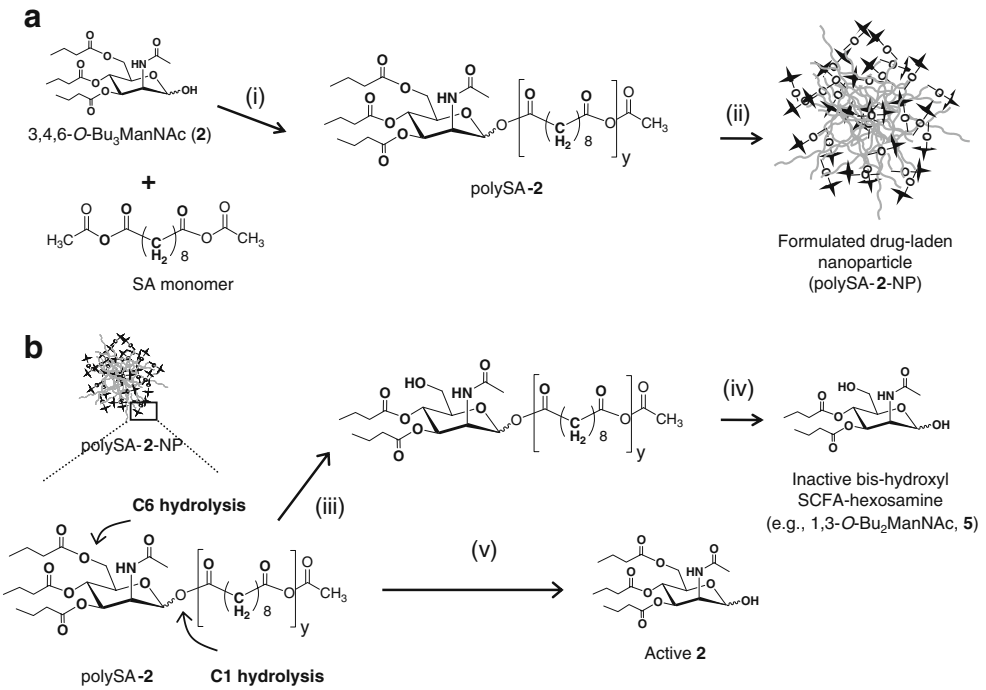

Fig. 6 Synthesis of polymer-linked 3,4-6-*O*-Bu_3ManNAc (2) and formulation into nanoparticles. **a** This scheme shows the strategy for (**i**) the synthesis of polySA-**2** by melt poly condensation and (**ii**) nanoparticle production by single emulsion solvent method. **b** Hydrolysis of 'active' **2** from polySA-**2**-NP must (**iii**) avoid initial hydrolysis of the C6-ester before (**iv**) the C1-ester is cleaved to release the analogue from the polymer; this scenario would generate **5**, a compound that lacks the signature of anti-cancer activities held by C6-SCFA derivatized analogs such as **1** and **2** [4, 5]. Instead, (**v**) hydrolysis of the C1 ester that links **2** to the polymer must occur before the hydrolysis of any of the other three ester-linked SCFA to achieve successful delivery of intact (*i.e.*, active) **2**

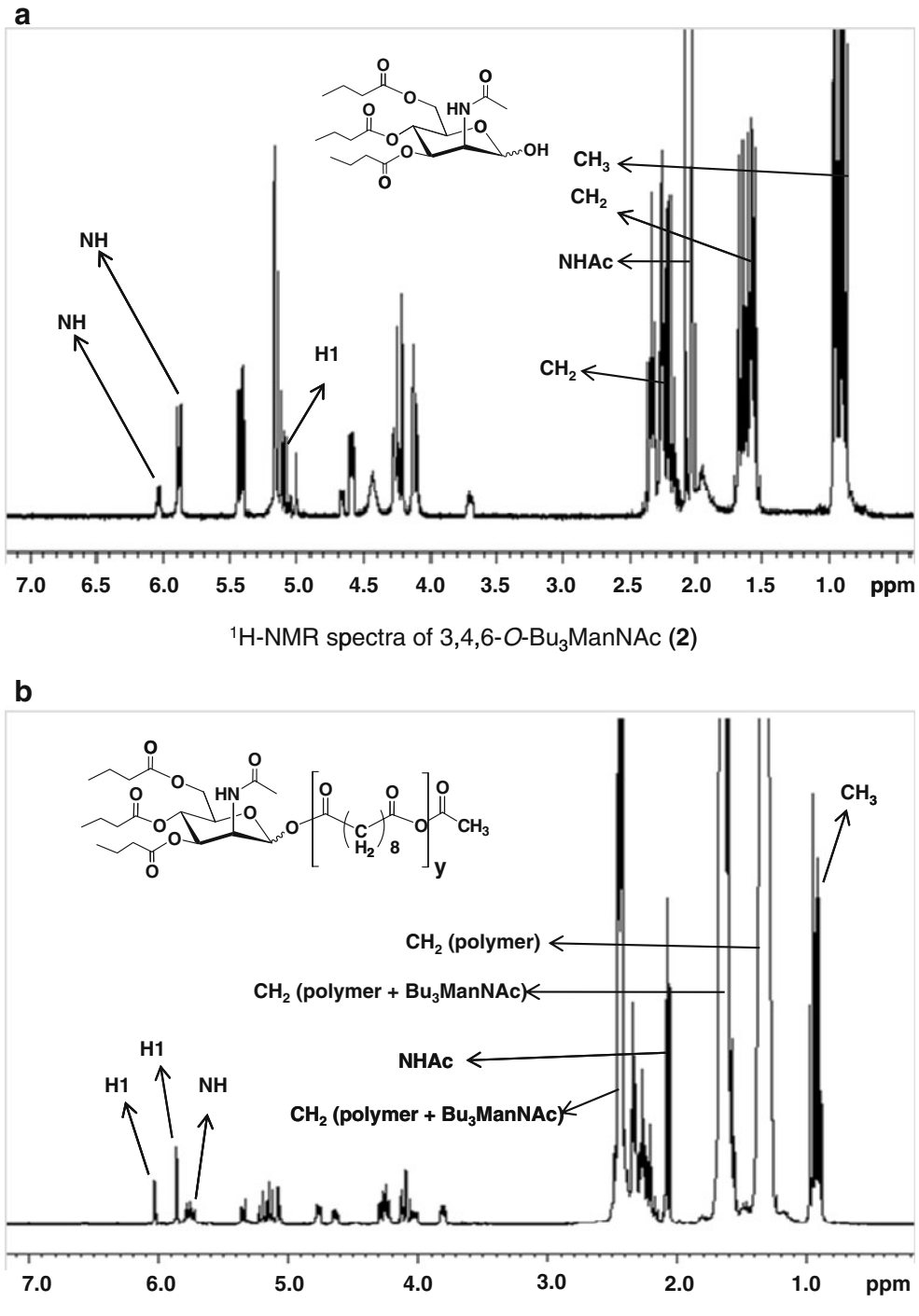

Fig. 7 Characterization of 2 after covalent conjugation to poly(PEG-SA). **a** ^{1}H-NMR (400 MHz, $CDCl_3$) spectrum of 2-acetamido-3,4,6-tri-*O*-butanoyl-2-deoxy-α,β-D-mannopyranose (**2**) **b** ^{1}H-NMR (400 MHz, $CDCl_3$) spectrum of 2-acetamido-3,4,6-tri-*O*-butanoyl-2-deoxy-α,β-D-mannopyranose (**2**) linked to poly(PEG-SA) (*i.e.*, "polySA-**2**")

degradation (Fig. 7). More substantially, the requirement existed that the C1-linkage be selectively hydrolyzed to release active **2** (as shown in Fig. 6, panel b) before the C3, C4, or C6 ester-linked SCFA were lost because, in the latter scenario, membrane-impermeable, relatively inactive bis-hydroxyl compounds (such as **4**, Fig. 1, panel a; or **5**, Fig. 6, panel b) would be generated upon eventual release of the C1 position. To confirm selective release through liberation of the C1-OH while retaining SCFA substitution at the C3, C4, and C6 positions, we evaluated the growth

inhibitory and cytotoxic properties of **2** in Jurkat cells. First, using concentrations of polySA-**2** matched with unconjugated **2** based on the 16% loading efficiency determined by NMR, growth was inhibited over 3 days and 5 days and resulted in cell death after 15 days; by contrast polySA did not inhibit growth nor was it cytotoxic. A similar response was elicited by polySA-**2**-NP (*i.e.*, polySA-**2** after formulation into nanoparticles); the drug-laden particles provided short term (3 day & 5 day) growth inhibition followed by cell death after 15 days; by comparison polySA-NP had minimal cytotoxicity (Fig. 8, panel b). These results are consistent with our previously-determined analysis of the biological activity of **2** [8, 10].

Characterization of the anti-cancer effects of polySA-**2**-NP in MDA-MB-231 Cells

To extend the evaluation of polySA-**2**-NP to a second cancer cell line and verify that the drug-laden nanoparticles supported the full range of biological and 'anti-cancer' responses elicited by unconjugated **2**, we tested the effects of this biomaterial on growth inhibition (Fig. 9, panel a) [8, 10], sialic acid production (panel b) [8, 10], and suppression of pro-invasive oncogenes (panel c; for comparison, the activity of unconjugated **2** on these genes is shown in panel d) [9]. The latter activity, the ability of C6-SCFA modified hexosamines to down-regulate MMP-9, CXCR-4, and NFKB1 (which together reduce the mobility of the metastatic breast cancer MDA-MB-231 line at subcytotoxic concentrations [9]) provides a highly promising avenue for cancer drug development but critically depends on the retention of the C6 acyl group during the drug delivery process (as outlined in Fig. 6, panel b). Therefore, it was important that these experiments demonstrated that SAR required for the attractive anticancer attributes of **2**, in particular the presence of a SCFA moiety at the C6-OH position [8], were retained upon covalent conjugation and release of the prodrug from polySA-**2**-NP.

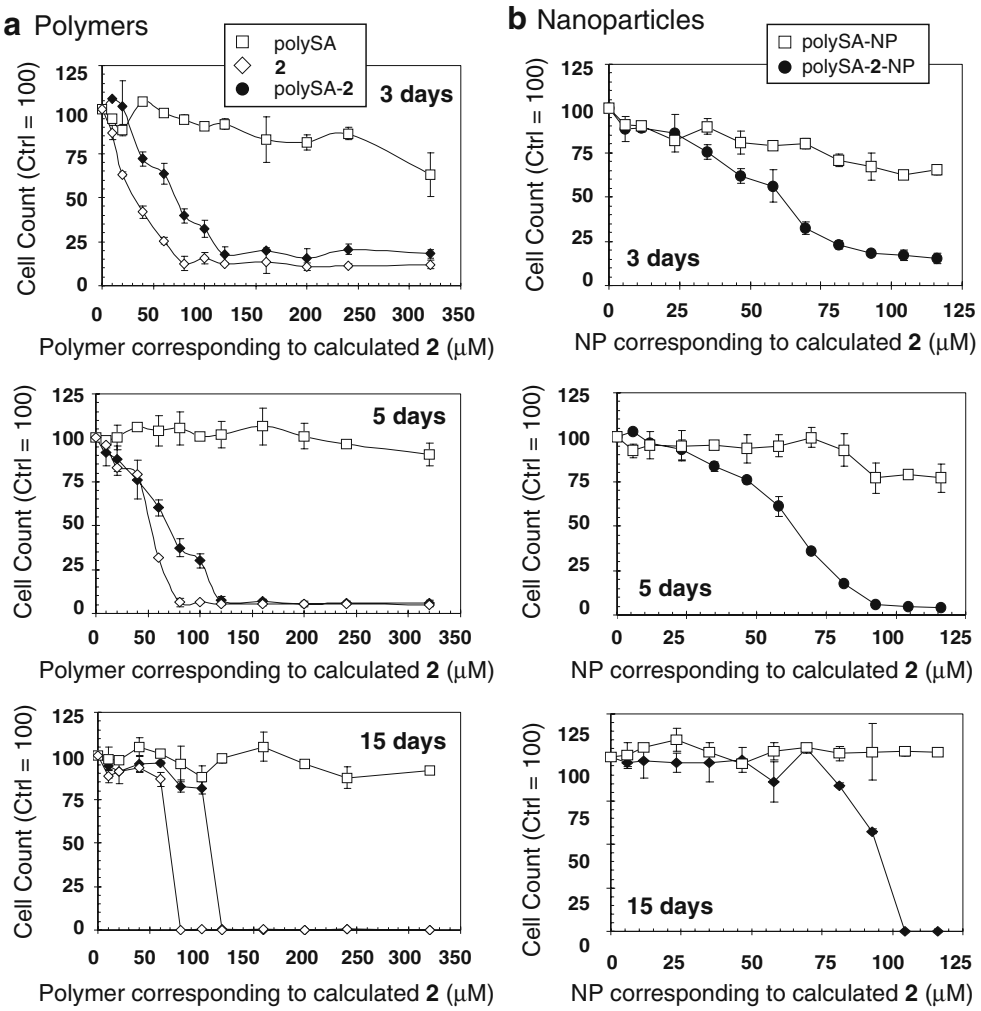

Fig. 8 Growth suppression and cytotoxicity of polySA-**2**. **a** Cell counts for Jurkat cells treated with of polySA-**2** and **b** polySA-**2**-NP; in both cases the relative number of cells compared to the untreated control is shown for 3 days, 5 days and 15 days (error bars represent SEM, $n \geq 3$) showing the progression from growth inhibition at early time points to complete cell death at 15 days that is characteristic for this class of analog (as described previously [6])

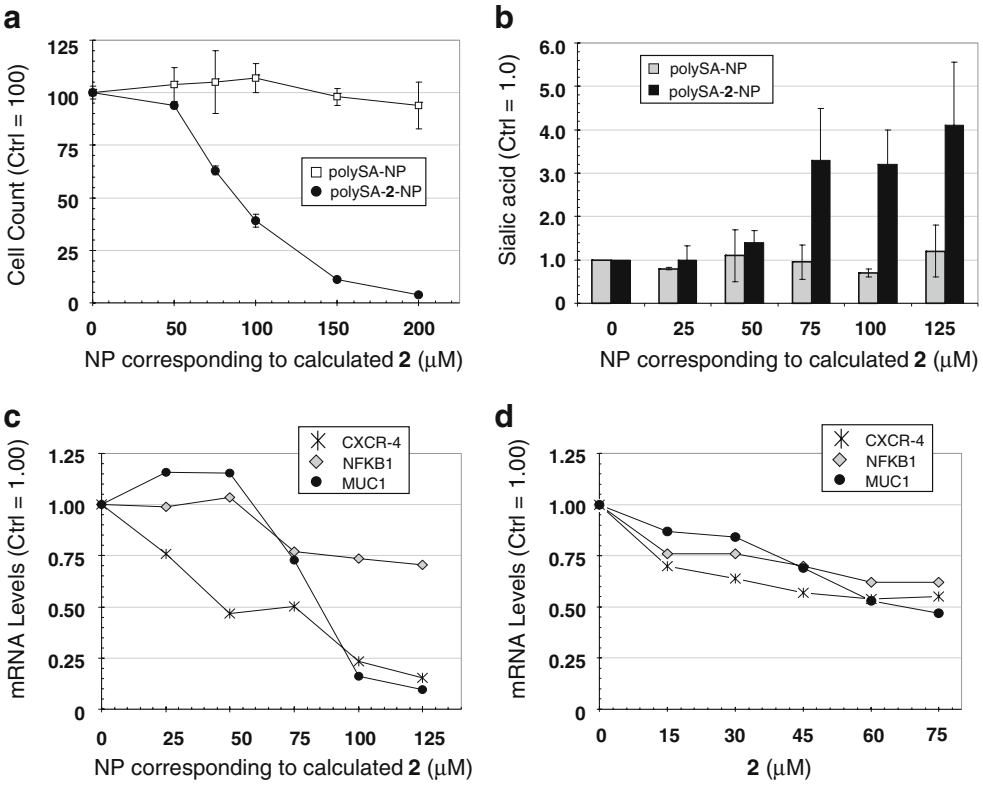

Fig. 9 'Anti-cancer' and biological effects of polySA-**2**-NP (and blank nanoparticles) in MDA-MB-231 cells. **a** Growth inhibition and **b** sialic acid production after 3 days of incubation with polySA-**2**-NP and polySA-**2**-NP are shown. For Panels **a** and **b**, error bars represent SEM ($n \geq 3$). **c** mRNA levels of pro-invasive oncogenes are suppressed by polySA-**2**-NP in a manner qualitatively similar to unconjugated **2**, as shown in Panel **d**. Data shown in Panels **c** and **d** represents qRT-PCR from a representative experiment (out of three independent experiments); each determination was based on four independent analyses (SEM was generally ≤2% for each data point and is not shown because the error bars were smaller than the symbol used to represent the data)

Summary and concluding comments

This study provides the groundwork for translating the growing interest in small molecule carbohydrate-based drugs (which are proving to be an unexpectedly versatile scaffold for drug discovery [2] and avoid heterogeneity and purity problems that plague larger carbohydrate-based therapeutics such as heparin [1]) into animal and clinical testing by demonstrating two methods for controlled release of butanoylated ManNAc. In one strategy, stable and controlled release over a multiday period was achieved by non-covalent encapsulation of Bu_4ManNAc **1** into microparticles made from non-toxic, surface-eroding PEG-SA polymer (*i.e.*, poly(PEG-SA):**1**). By offering improved biological activity (*e.g.*, prolonged and increased sialic acid production), this biomaterial lays a beneficial foundation for both *in vitro* metabolic glycoengineering efforts and for *in vivo* therapeutic use. To provide an illustrative *in vitro* application, the increased efficiency of sialic acid production afforded by controlled release may pay dividends for recombinant glycoprotein production, where media supplementation with SCFA-hexosamines can increase produce quality [12] and the installation of non-natural sugar epitopes improves pharmacologic properties [25]. When extrapolated to the industrial scale, savings of 30–40% (*i.e.*, approximately the gain in efficiency seen in this study) in the cost of SCFA-monosaccharides used for metabolic glycoengineering applications would be substantial.

For *in vivo* and therapeutic applications, the prolonged release of **1** from poly(PEG-SA):**1** offers the means to reduce the currently-employed twice daily injection protocols [16] to once a week administration. In addition to providing less invasive routine administration, the controlled release from drug laden polymer opens the door to new therapeutic uses such as surgical implantation into the brain for treatment of glioma if formulated into appropriate wafers. Importantly, the therapeutic possibilities for SCFA-hexosamine delivery were significantly expanded by the second approach where **2** was shown to maintain biological activity after covalent linkage to polymeric polySA and formulation into nanoparticles. In the future additional gains in efficiency are anticipated from sizing the nanoparticles for efficient cell uptake and installing surface functionalities such as antibodies that recognize tumor associated antigens to target the particles to the specific classes of disease cells. In summary, the results of these studies establish a framework for *in vivo* delivery of carbohydrate-based drug candidates, a class of molecules with considerable therapeutic potential once their poor pharmacological properties are overcome through strategies such as those described in this report.

Materials and methods

Synthesis of **1** and **2**

The synthesis, purification, and characterization of Bu_4ManNAc (**1**, 2-acetamido-2-deoxy-1,3,4,6-tetra-*O*-butanoyl-α,β-D-mannopyranose) and 3,4,6-*O*-Bu_3ManNAc (**2**, 2-acetamido-3,4,6-tri-*O*-butanoyl-2-deoxy-α,β-D-mannopyranoses) followed published procedures [7, 8]. NMR spectra of **2** are provided in Figs. S1–S3 of the Supplementary Material.

Synthesis and characterization of poly(PEG-SA)

The synthesis of poly(PEG-SA) (10% PEG and 90% SA) followed the procedure previously reported by Fu and coworkers [17]. Briefly, sebacic acid prepolymer was made by reflux of sebacic acid in acetic anhydride followed by drying by rotary evaporation, recrystallization from dry toluene, and washing with 1:1 anhydrous ethyl ether: petroleum ether. PEG prepolymer was made by reflux of polyoxyethylene dicarboxylic acid in acetic anhydride, removal of the solvent by rotary evaporation, and extraction with anhydrous ether. The poly(PEG-SA) co-block polymer was then synthesized by the melt polycondensation method and characterized by proton NMR and FT-IR [17].

The molecular weight and polydispersity of PEG-SA were determined by gel permeation chromatography (GPC) analysis (JASCO PU-980 intelligent HPLC pump, 1560 intelligent column thermoset, RI-1530 intelligent refractive index detector). Samples were filtered and eluted in chloroform through a series of Styragel columns (guard, HR4, and HR3 Waters Styragel columns) at a flow rate of 0.3 mL/min. The molecular weights were determined relative to polystyrene standards (Fluka, Milwaukee, WI). These parameters were determined to be: M_w=41000; M_n= 18000; and PDI=2.22.

Encapsulation of **1** in poly(PEG-SA) and microparticle formulation

Encapsulation of Bu_4ManNAc (**1**) in poly(PEG-SA) (to prepare polymer-encapsulated **1** subsequently referred to as poly(PEG-SA):**1**) followed the melt polycondensation method described above for SA and PEG prepolymers but with the inclusion of **1** at starting ratios of poly(PEG-SA) to **1** of 70:30 and 80:20 by weight. Subsequently, microparticles were prepared using a double emulsion solvent evaporation method [17]. Briefly, Bu_4ManNAc and PEG-SA were dissolved in chloroform (50 mg/mL) and emulsified into a 1.0% w/w poly(vinyl alcohol) (M_w=25000, Polysciences, Warrington, PA) aqueous solution using a Silverson homogenizer at 4000 RPM for 2.0 min (L4RT, Silverson Machines, East Longmeadow, MA). Particles were hardened by allowing chloroform to evaporate at room temperature while stirring for 2.0 h. Particles were collected and washed three times with double distilled water via centrifugation at 2,600×*g* for 15 min (International Equipment Co., Needham Heights, MA). Particle size distribution was determined using a Coulter Multisizer IIe (Beckman). Particles were re-suspended in double distilled water and added dropwise to 100 mL of ISOTON II diluents (Beckman) until the coincidence of the particles was between 8.0% and 10%. The mass-average size distribution of microparticles was determined by analyzing $\geq 10^5$ particles, which were sized for each batch using a Coulter Multisizer IIe [17].

HPLC characterization of Bu_4ManNAc anomers (**1α** and **1β**)

A stock solution of **1** in acetonitrile was prepared and aliquots were analyzed by HPLC. HPLC measurements were conducted using a reversed-phase Nova-Pak® C_{18} column (Waters, MA, WAT086344, 4 μm, 3.9×150 mm), under isocratic conditions at a flow rate of 0.5 mL/min. A solution of **1** (10 mg/mL in acetonitrile) was injected into a HPLC system (Waters delta 600 pump equipped with a PDA (photo diode array) 2996 and RI 2412 detection system using a reverse phase column) and detected at a wavelength (λ) of 210 nm using the PDA. The amide excitation wavelength of 210 nm has been previously used for the detection of amino-containing carbohydrates, particularly sialic acids [26]. The eluant of 3:1 acetonitrile:water was selected based on baseline quality and the ability to separate a mixture of α- and β-anomers under isocratic conditions. A flow rate of 0.5 mL/min at 22°C was used and at least three replicate runs were performed for all samples. For **1**, which consists of a mixture of α- and β-anomers after synthesis and column isolation, each anomer could be distinguished by their relative retention times and the 90:10 ratio of anomers was in accordance with the published ^{1}H-NMR data [7].

Determination of the solubility of Bu_4ManNAc in PBS at 37°C

Bu_4ManNAc (**1**, 10 mg) was suspended in PBS (1.0 mL) and maintained at 37°C. After allowing equilibrium to occur over 16 h, the supernatant was carefully taken in a micro syringe and injected for HPLC analysis as described above. Multiple injections were performed to obtain statistically significant estimates of area under the curve (AUC). The AUC was calibrated using the acetonitrile-

derived standard curve to find the saturating concentration of Bu_4ManNAc in PBS at 37°C.

HPLC quantification of controlled release of Bu_4ManNAc (**1**)

Three replicate samples of 10 mg of poly(PEG-SA):**1** microparticles were suspended in phosphate buffered saline (PBS) (1.0 mL) were incubated at 37°C. At various time intervals, the suspension was centrifuged (16100×*g*) to pellet the intact microparticles. The supernatants were carefully removed and placed in fresh 1.5 mL microcentrifuge tubes and stored at −20°C until analysis. The residual microparticles were re-suspended with fresh PBS (1.0 mL) and incubation at 37°C was continued until the next time point 24 h later. Frozen aliquots of supernatants were thawed at 37°C for 15 min before HPLC analysis and the concentration of **1** was estimated by calibration with the standard curve. The total amount of **1** released from the particles was calculated based on HPLC quantification by summation of data from each day; the cumulative total of analog released over the first 12 days provided an estimate of the efficiency of encapsulation (which was 78:22 for a starting ratio of 70:30 and 88:12 for a starting ratio of 80:20).

Growth inhibition and cytotoxicity assays

The growth inhibitory properties of *n*-butanoylated hexosamines have been studied extensively and cell counts at early (*e.g.*, after 3–5 days of exposure to a single addition of compound to the culture medium) and later (*e.g.*, after 15 days) time points have proven to be reliable indicators of HDACi-associated growth inhibition and apoptosis, respectively [10]. Consequently, in this study, cell counts obtained using a Coulter Counter Z2 particle sizing instrument were routinely used to monitor cytotoxicity as an indicator of the biological activity of **1** after encapsulation as poly(PEG-SA):**1** and subsequent release. In a typical experiment, cells were incubated with unencapsulated **1** (*i.e.*, the positive control), unconjugated polymer microparticles (*i.e.*, the negative control), or poly(PEG-SA):**1** (or conjugated **2**; *i.e.*, the test compounds). In all cases, cell counts were compared with solvent-treated controls; in particular, because stock solutions of **1** were prepared in EtOH (to maintain sterility and assist solubility), the culture medium for all cell-based assays were adjusted to contain the same amount of ethanol as the test well with the highest level of **1**. It should be noted that this control was done simply as a precaution, because the amount of EtOH used was less than 0.4% (v/v), a level that previous studies have showed had no noticeable effect on the biological endpoints under evaluation [10, 20, 27].

A functional assay was used for monitoring sialic acid production from polymer-released **1**

Sialic acid production is an unambiguous endpoint to monitor the biological activity of polymer-delivered ManNAc analogs because this sugar is dedicated to sialic acid biosynthesis with no other known metabolic fates [21, 22]; accordingly, a previously developed functional assay [20] using indicator cells was employed to evaluate poly(PEG-SA):**1**. In these experiments, Jurkat cells grown in RPMI-1640 medium with 5.0% FBS, penicillin, and streptomycin were incubated (i) without analog (but with a 1:10 addition of blank PBS for consistency with the medium conditions in (ii) and (iii)); (ii) with supernatants from PBS-incubated poly(PEG-SA):**1** containing the released analog (after a 1:10 dilution in cell culture medium); or (iii) with stock solutions of analog (*i.e.*, unencapsulated **1**) at concentrations corresponding to those found in the particle-released supernatants based on HPLC quantification. The cells were harvested after 48 h of incubation, counted, washed twice with PBS, re-suspended in 300 μL of PBS and lysed by three freeze-thaw cycles. The lysates were analyzed for sialic acid content by the colorimetric periodate-resorcinol assay following reported procedures [28] and adapted for microplate or mini-cuvette format [20, 29]. Sialic acid levels were normalized against the total number of cells present at the end of the culture period and the data was presented as the number of sialic acid molecules per cell.

Sialic acid production from poly(PEG-SA):**1** after formulation into microparticles

The next experiments were designed to confirm that poly (PEG-SA):**1** retained biological activity when the drug laden microparticles were added directly to cell cultures. In these experiments, 'empty' polymer (poly(PEG-SA)) microparticles were used as the negative control and unencapsulated **1** served as the positive control. The functional assays followed the general procedure described above for evaluation of pre-released **1** where the test compounds were added to the indicator cells on Day 0. In these assays, however, aliquots of cells were removed periodically for analysis (typically, on Day 1, 3, 5, 7, 9, and 11). In order to keep the remaining cells—to be analyzed on subsequent days—in the robust growth phase required for optimal sialic acid production (as previously described [20]), the cell densities of the samples were adjusted to ~2.5 x10^5 cells/mL by adding back an appropriately calculated amount of fresh medium on alternate days starting from day 5 until day 11.

In this set of assays, the similarity in size between the microparticles (8 μm) and Jurkat cells (7–15 μm) had the

potential to introduce artifacts into cell counts. Accordingly, the sialic acid content was normalized against total protein concentration rather than against number of cells as is typically done in our experiments [7, 10, 27, 29]. Briefly, the cells from the harvested aliquots were washed with PBS to remove residual serum glycoprotein and re-suspended in PBS, lysed by freeze/thaw cycles, and centrifuged (16,100×*g*, 1.0 min). The supernatant from each sample was then divided for total sialic acid estimation using periodate-resorcinol assay (as described above, using 300 μL) and for protein estimation by microBCA assay (using 150 μL) (Pierce, Rockford, IL). In these experiments, the amount of sialic acid was normalized against protein concentration and presented as nanograms of sialic acid per microgram of protein.

Synthesis of polySA-**2**

Next, polySA with covalently attached 3,4,6-*O*-Bu_3ManNAc (denoted "polySA-**2**") was prepared. First, the tributanolylated analog 3,4,6-*O*-Bu_3ManNAc (**2**) was synthesized and characterized as reported previously [8] and the strategy outlined in Figure 6 then was used to covalently attach **2** to polySA. Briefly, polySA was prepared by melt polycondensation of **2** and sebacic acid prepolymer at 180°C under high vacuum, precipitated from chloroform into petroleum ether, and dried by vacuum [17]. NMR and FT-IR characterization of compound **2** and polySA-**2** verified the presence of the analog covalently attached to the polymer.

*Characterization of 2-acetamido-3,4,6-tri-O-butanoyl-2-deoxy-α,β-D-mannopyranose, 3,4,6-O-Bu_3ManNAc (**2**)* Crystalline solid (mixture of anomers, major : minor=88 : 12): IR (ν, cm^{-1}): 2927.0, 2911.4, 2868.9, 2849.9, 1800.1, 1740.1, 1527.2, 1469.9, 1411.1, 1380.3, 1358.3, 1305.4, 1284.4, 1249.7, 1204.0, 1168.0, 1076.1, 1040.0, 902.7, 869.9, 755.2, 721.6.; ^{1}H-NMR (400 MHz, $CDCl_3$): δ 6.04 (d, 0.12H, *J*=8.4 Hz, NH), 5.88 (d, 0.88H, *J*=8.8 Hz, NH), 5.42 (dd, 0.88H, *J*=4.4 and 10.0 Hz), 5.22–5.02 (m, 2.12 H), 5.00 (s, 0.12H) 4.65 (m, 0.12H, H-2), 4.58 (m, 0.88H, H-2), 4.43 (m, 0.88H) 4.32–4.05 (m, 2.88H), 3.70 (m, 0.12H, H-5), 2.45–2.13 (m, 6H), 2.10 (s, 0.36H, NHAc), 2.05 (s, 2.64H, NHAc), 1.90–1.50 (m, 6H), 1.10–0.80 (m, 9H); ^{13}C-NMR (100 MHz, $CDCl_3$) : δ 173.6, 173.2, 173.0, 173.0, 172.9, 172.8, 171.2 (NHCO), 171.2 (NHCO), 94.1 (C-1), 93.8 (C-1), 73.0, 72.0, 69.3, 68.4, 66.8, 66.0, 62.8 (C-6), 62.8 (C-6), 52.4 (C-2), 51.8 (C-2), 36.4, 36.4, 36.3, 23.6, 18.7, 18.7, 18.5, 14.0, 14.0, 14.0.

*Characterization of polymer-3,4,6-O-Bu_3ManNAc (polySA-**2**)* IR (ν, cm^{-1}): 3359.1, 3258.1, 2965.5, 2877.1, 2359.9, 1737.5, 1653.6, 1540.6, 1417.4, 1372.5, 1293.3, 1262.1, 1185.9, 1108.1, 1078.0, 1028.1, 984.4, 795.1, 699.4.; ^{1}H-NMR (400 MHz, $CDCl_3$): δ 6.04 (d, 0.40 H, *J*=1.6 Hz, H-1 minor), 5.87 (d, 0.60 H, *J*=2 Hz, H-1 major), 5.80–5.74 (1H, two doublet, NH), 5.34 (dd, 0.40 H, *J*=4.4 and 10.0 Hz), 5.21–5.02 (m, 2.60 H), 5.00 (s, 0.12H) 4.77 (m, 0.60H, H-2), 4.63 (m, 0.40H, H-2), 4.32–4.05 (m, 2.40H), 3.80 (m, 0.60H, H-5), 2.55–2.10 (m, 140H), 2.09 (s, 3H, NHAc), 1.78–1.50 (m, 140 H {6H + polymer H}), 1.45–1.20 (m, 248 H, polymer H), 1.00–0.80 (m, 12H); ^{13}C-NMR (100 MHz, $CDCl_3$) : δ 173.1, 172.4, 172.4, 172.1, 171.1, 170.8, 170.3, 171.0, 169.5, 169.5, 91.7 (C-1), 90.7 (C-1), 73.7, 71.2, 70.4, 68.8, 65.3,61.9 (C-6), 61.8 (C-6), 49.8 (C-2), 49.4 (C-2), 35.4, 35.4, 35.0, 34.0, 33.9, 33.6, 29.8, 28.9, 28.7, 28.6, 28.6, 28.4, 24.7, 24.0, 23.3, 10.4, 10.4, 10.3, 10.1.

Formulation of polySA-**2** into nanoparticles (polySA-**2**-NP)

Nanoparticles formulated from polySA-**2** (denoted *"of polySA-2-NP")* were prepared using the single emulsion solvent method. Briefly, 10 mg of polySA-**2** was dissolved in 2.0 mL of dichloromethane to produce a 5.0 mg/mL solution. Poly(vinyl alcohol) (PVA) (M_w=25000, 88% hydrolyzed) was dissolved in distilled water to make 0.1% and 1.0% solutions. The polySA-**2** solution was then added to 4.0 mL of 1.0% PVA, sonicated for 3.0 min, and then poured into 40 mL of 0.1% PVA and stirred for an additional 3.0 h to allow the dichloromethane to evaporate. Particles were concentrated by rotavap, than dialyzed into water. Nanoparticle size analysis was performed by Dynamic Light Scattering (DLS) using a Zetasizer ® 3000 (Malvern Instruments Inc., Southborough, MA) with the sample diluted in filtered distilled water. The measurements were performed at 25°C at a scattering angle of 90°. PolySA nanoparticles without conjugated **2** were made by using the same methodology, but beginning with polySA rather than polySA-**2**.

Biological evaluation of polySA-**2** and polySA-**2**-NP

To ensure that **2** delivered from polySA-**2** and polySA-**2**-NP retained biological activity, the growth inhibitory properties of these materials were evaluated in Jurkat cells in tandem with the appropriated controls (*e.g.*, unencapsulated **2** and unladen polymer) by using the methods described above. Then, to verify that these effects extended to other cell types, growth inhibition (and sialic acid production, again as described above), were evaluated in the human breast cancer MDA-MB-231 line. Finally, to ensure that polymer-delivered **2** retained the 'scaffold-dependent' anti-cancer activities (as described in detail elsewhere [3, 8, 9]), mRNA levels of the pro-invasive

oncogenes CXCR-4, NFKB1, and MUC1 were evaluated by quantitative real-time PCR (qRT-PCR) using published methods [9].

Acknowledgments Funding for this project was provided by the National Institutes of Health (CA11231404) for SCFA-hexosamine synthesis and analysis of anti-metastatic responses in MDA-MB-231 cells, (EB005692-03 for synthesis and evaluation of sebacic acid-PEG polymers), and the Johns Hopkins Institute for NanoBioTechnology (INBT, for the synthesis and biological evaluation of the covalently-conjugated nanoparticles).

References

1. Liu, H., Zhang, Z., Linhardt, R.J.: Lessons learned from the contamination of heparin. Nat. Prod. Rep. **26**, 313–321 (2009)
2. Meutermans, W., Le, G.T., Becker, B.: Carbohydrates as scaffolds in drug discovery. ChemMedChem **1**, 1164–1194 (2006)
3. Elmouelhi, N., Aich, U., Paruchuri, V.D.P., Meledeo, M.A., Campbell, C.T., Wang, J.J., Srinivas, R., Khanna, H.S., Yarema, K.J.: Hexosamine template. A platform for modulating gene expression and for sugar-based drug discovery. J. Med. Chem. **52**, 2515–2530 (2009)
4. Kayser, H., Zeitler, R., Kannicht, C., Grunow, D., Nuck, R., Reutter, W.: Biosynthesis of a nonphysiological sialic acid in different rat organs, using *N*-propanoyl-D-hexosamines as precursors. J. Biol. Chem. **267**, 16934–16938 (1992)
5. Du, J., Meledeo, M.A., Wang, Z., Khanna, H.S., Paruchuri, V.D., Yarema, K.J.: Metabolic glycoengineering: Sialic acid and beyond. Glycobiology **19**, 1382–1401 (2009)
6. Sarkar, A.K., Fritz, T.A., Taylor, W.H., Esko, J.D.: Disaccharide uptake and priming in animal cells: inhibition of sialyl Lewis X by acetylated Gal β1, 4GlcNAc β-O-naphthalenemethanol. Proc. Natl. Acad. Sci. U.S.A. **92**, 3323–3327 (1995)
7. Kim, E.J., Sampathkumar, S.-G., Jones, M.B., Rhee, J.K., Baskaran, G., Yarema, K.J.: Characterization of the metabolic flux and apoptotic effects of *O*-hydroxyl- and *N*-acetylmannosamine (ManNAc) analogs in Jurkat (human T-lymphoma-derived) cells. J. Biol. Chem. **279**, 18342–18352 (2004)
8. Aich, U., Campbell, C.T., Elmouelhi, N., Weier, C.A., Sampathkumar, S.-G., Choi, S.S., Yarema, K.J.: Regioisomeric SCFA attachment to hexosamines separates metabolic flux from cytotoxcity and MUC1 suppression. ACS Chem. Biol. **3**, 230–240 (2008)
9. Campbell, C.T., Aich, U., Weier, C.A., Wang, J.J., Choi, S.S., Wen, M.M., Maisel, K., Sampathkumar, S.-G., Yarema, K.J.: Targeting pro-invasive oncogenes with short chain fatty acid-hexosamine analogs inhibits the mobility of metastatic MDA-MB-231 breast cancer cell. J. Med. Chem. **51**, 8135–8147 (2008)
10. Sampathkumar, S.-G., Jones, M.B., Meledeo, M.A., Campbell, C.T., Choi, S.S., Hida, K., Gomutputra, P., Sheh, A., Gilmartin, T., Head, S.R., Yarema, K.J.: Targeting glycosylation pathways and the cell cycle: sugar- dependent activity of butyrate-carbohydrate cancer prodrugs. Chem. Biol. **13**, 1265–1275 (2006)
11. Wang, Z., Du, J., Che, P.-L., Meledeo, M.A., Yarema, K.J.: Hexosamine analogs: from metabolic glycoengineering to drug discovery. Curr. Opin. Chem. Biol. **13**, 565–572 (2009)
12. Viswanathan, K., Lawrence, S., Hinderlich, S., Yarema, K.J., Lee, Y.C., Betenbaugh, M.: Engineering sialic acid synthetic ability into insect cells: identifying metabolic bottlenecks and devising strategies to overcome them. Biochemistry **42**, 15215–15225 (2003)
13. Campbell, C.T., Sampathkumar, S.-G., Weier, C., Yarema, K.J.: Metabolic oligosaccharide engineering: perspectives, applications, and future directions. Mol. Biosyst. **3**, 187–194 (2007)
14. Aich, U., Yarema, K.J.: Metabolic oligosaccharide engineering: perspectives, applications, and future directions. In: Fraser-Reid, B., Tatsuta, K., Thiem, J. (eds.) Glycosciences, 2nd edn, pp. 2136–2190. Springer-Verlag, Berlin (2008)
15. Sarkar, A.K., Brown, J.R., Esko, J.D.: Synthesis and glycan priming activity of acetylated disaccharides. Carbohydr. Res. **329**, 287–300 (2000)
16. Gagiannis, D., Gossrau, R., Reutter, W., Zimmermann-Kordmann, M., Horstkorte, R.: Engineering the sialic acid in organs of mice using N-propanoylmannosamine. Biochim. Biophys. Acta **1770**, 297–306 (2007)
17. Fu, J., Fiegel, J., Krauland, E., Hanes, J.: New polymeric carriers for controlled drug delivery following inhalation or injection. Biomaterials **23**, 4425–4433 (2002)
18. Zhang, I., Gu, F.X., Chan, J.M., Wang, A.Z., Langer, R.S., Farokhzad, O.C.: Nanoparticles in medicine: therapeutic applications and developments. Clin. Pharmacol. Ther. **83**, 761–769 (2008)
19. Quick, D.J., Macdonald, K.K., Anseth, K.S.: Delivering DNA from photocrosslinked, surface eroding polyanhydrides. J. Control. Release **97**, 333–343 (2004)
20. Jones, M.B., Teng, H., Rhee, J.K., Baskaran, G., Lahar, N., Yarema, K.J.: Characterization of the cellular uptake and metabolic conversion of acetylated *N*-acetylmannosamine (ManNAc) analogues to sialic acids. Biotechnol. Bioeng. **85**, 394–405 (2004)
21. Tanner, M.E.: The enzymes of sialic acid biosynthesis. Bioorg. Chem. **33**, 216–228 (2005)
22. Luchansky, S.J., Yarema, K.J., Takahashi, S., Bertozzi, C.R.: GlcNAc 2-epimerase can serve a catabolic role in sialic acid metabolism. J. Biol. Chem. **278**, 8036–8042 (2003)
23. Sampathkumar, S.-G., Campbell, C.T., Weier, C., Yarema, K.J.: Short-chain fatty acid-hexosamine cancer prodrugs: the sugar matters! Drug. Future **31**, 1099–1116 (2006)
24. Lavis, L.D.: Ester bonds in prodrugs. ACS Chem. Biol. **3**, 203–206 (2008)
25. Luchansky, S.J., Argade, S., Hayes, B.K., Bertozzi, C.R.: Metabolic functionalization of recombinant glycoproteins. Biochemistry **43**, 12358–12366 (2004)
26. Whalen, M.M., Wild, G.C., Spall, W.D., Sebring, R.J.: Separation of underivatized gangliosides by ion exchange high performance liquid chromatography. Lipids **21**, 267–270 (1986)
27. Kim, E.J., Jones, M.B., Rhee, J.K., Sampathkumar, S.-G., Yarema, K.J.: Establishment of *N*-acetylmannosamine (ManNAc) analogue-resistant cell lines as improved hosts for sialic acid engineering applications. Biotechnol. Prog. **20**, 1674–1682 (2004)
28. Jourdian, G.W., Dean, L., Roseman, S.: The sialic acids. XI. A periodate-resorcinol method for the quantitative estimation of free sialic acids and their glycosides. J. Biol. Chem. **246**, 430–435 (1971)
29. Yarema, K.J., Goon, S., Bertozzi, C.R.: Metabolic selection of glycosylation defects in human cells. Nat. Biotechnol. **19**, 553–558 (2001)